Inorganic Chemistry Communications 181 (2025) 115060

Contents lists available at ScienceDirect

Inorganic Chemistry Communications

journal homepage: www.elsevier.com/locate/inoche

Research Article

Curcumin-coated Sr/Co-doped TiO_2 nanoparticles: Synthesis, characterization, and evaluation of antimicrobial, antioxidant, and anticancer activities against liver cancer cells

Shivangi Gupta [a,*], R. Roopashree [b], Vivek Saraswat [c], Shivangi Giri [d], Jagmeet Sohal [e], Thalakulam Shanmugam Boopathi [f,g], Fatimah S. Al-Khattaf [h], Ashraf Atef Hatamleh [h], Tingting Qiao [i]

[a] Quantum University Research Center, Quantum University, Roorkee 247667, Uttarakhand, India
[b] Department of Chemistry and Biochemistry, JAIN (Deemed-to-be University), Bangalore 560002, Karnataka, India
[c] Centre of Research Impact and Outcome, Chitkara University, Rajpura 140417, Punjab, India
[d] Department of Sciences, Vivekananda Global University, Jaipur 303012, India
[e] Chitkara Centre for Research and Development, Chitkara University, Himachal Pradesh 174103, India
[f] Department of Chemistry, Amrita School of Physical Sciences, Coimbatore, Amrita Vishwa Vidyapeetham, 641112, India
[g] Functional Materials Laboratory, Amrita School of Engineering, Coimbatore, Amrita Vishwa Vidyapeetham, 641112, India
[h] Department of Botany and Microbiology, College of Science, King Saud University, P.O. Box 2455, Riyadh 11451, Saudi Arabia
[i] School of Business Administration, Shenyang Pharmaceutical University, Shenyang 110016, China

ARTICLE INFO

Keywords:
TiO_2
Curcumin
Antibacterial
Antifungal
Anticancer
Antioxidant activity
Ion-doping

ABSTRACT

In this study, a novel curcumin-coated, Sr and Co co-doped TiO_2 (TiO_2SrCoCur) nanoparticles (NPs) was synthesized via a sol-gel method and extensively characterized for its structural, morphological, optical, and antibacterial properties. XRD confirmed the anatase phase of TiO_2 with successful doping of Sr and Co, while FTIR and XPS analyses validated the presence of curcumin and functional surface groups. TEM analysis revealed spherical particles with an average size of approximately 36 nm, whereas DLS showed a larger hydrodynamic diameter of ~224 nm due to agglomeration and solvation effects. UV–Vis spectroscopy exhibited characteristic absorption peaks at 230 and 286 nm, confirming the optical transitions influenced by doping and curcumin interaction. The TiO_2SrCoCur NPs showed enhanced antibacterial activity against G+ and G- bacteria (*S. aureus, B. subtilis, B. megaterium, K. pneumoniae, P. valgaris,* and *V. cholerae*) and antifungal activity against *C. albicans.* Additionally, anticancer property against liver cancer HePG-2 cells is also studied, which shows significant cytotoxicity with IC50 of ~7 μg/mL. A reasonable level of antioxidant activity is found when the Trolox equivalent study is used for analysis. As a result, the as-synthesized curcumin-coated Sr/Co-doped TiO_2 NPs show adequate biocidal properties to be used as effective therapeutic agents against pathogenic bacteria, fungi, and liver cancer treatment applications.

1. Introduction

Liver cancer, particularly hepatocellular carcinoma (HCC), is a leading cause of cancer-related deaths, often linked to chronic liver diseases like cirrhosis, hepatitis B/C, and excessive alcohol use. Symptoms are usually subtle, and as the disease progresses, it can lead to liver failure and metastasis, making treatment challenging [1]. Current therapies like surgery and chemotherapy have limitations, including high recurrence rates and severe side effects, necessitating more effective, targeted solutions. Nanotechnology presents a promising alternative, with nanoparticles enhancing drug delivery to cancer cells while minimizing toxicity [2]. Additionally, nanoparticles can be functionalized with targeting ligands for precise delivery and possess antibacterial and antifungal properties, offering protection against infections in immunocompromised patients. TiO_2-based nanoparticles, for example, have dual anticancer and antimicrobial effects, inducing oxidative stress in cancer cells while preventing infections. Their ability for controlled drug release further improves treatment efficacy and

* Corresponding author:
E-mail address: shivangi.gupta@quantumeducation.in (S. Gupta).

https://doi.org/10.1016/j.inoche.2025.115060
Received 22 January 2025; Received in revised form 6 July 2025; Accepted 7 July 2025
Available online 9 July 2025

patient compliance, positioning nanotechnology as a powerful tool in liver cancer therapy [3].

TiO_2 NPs offer significant advantages in biomedical applications, such as drug delivery, biosensing, photodynamic therapy, and cancer treatment, owing to their unique properties, including non-toxicity, abundance, and tunable size and surface characteristics. Anatase TiO_2, in particular, shows higher photocatalytic and biological activity compared to the rutile form, making it effective in combating bacterial and fungal infections, promoting wound healing, and providing antioxidant and anticancer properties. However, while TiO_2 NPs have shown promise, there are notable drawbacks when used alone. Pure TiO_2 NPs often exhibit limited biocompatibility and can be relatively biocidal to normal cells, which raises concerns regarding their safety in therapeutic applications. Additionally, TiO_2 NPs tend to have low photocatalytic efficiency under visible light and may not produce sufficient reactive oxygen species (ROS) to induce the desired therapeutic effects [4–10].

To overcome these limitations, researchers have explored doping TiO_2 NPs with various elements, such as metal and non-metal dopants, to enhance their performance. Doping improves the photocatalytic activity of TiO_2 under visible light, increases their antimicrobial and anticancer efficacy, and enhances their biocompatibility by reducing cytotoxicity. By modifying the crystal structure, electronic properties, and surface defects of TiO_2, dopants can tailor the material for specific biomedical applications. This makes TiO2-based nanocomposites and bio-nanocomposites a more effective solution for combating infections, treating cancer, and addressing other biomedical challenges. Thus, doping TiO2 NPs is essential to expanding their range of applications while minimizing potential adverse effects, ensuring their safety and efficacy in medical treatments [11–15].

Strontium (Sr) and cobalt (Co) are excellent dopants for TiO_2 NPs in biomedical applications due to their unique properties that enhance TiO_2's performance in various therapeutic contexts. Strontium is widely recognized for its beneficial effects on bone health, promoting osteoblast differentiation and mineralization, which makes it a valuable dopant for bone regeneration and tissue engineering applications. Additionally, Sr doping improves the biocompatibility of TiO_2, reducing cytotoxicity and inflammation, which is critical for biomedical devices in direct contact with living tissues. Strontium also possesses antimicrobial properties, which can enhance TiO_2's ability to prevent infections in medical implants and support wound healing. On the other hand, cobalt is known for its catalytic and antimicrobial properties, enhancing TiO_2's photocatalytic activity and ability to generate reactive oxygen species (ROS), making it more effective in photodynamic therapy and microbial disinfection. Cobalt doping also boosts TiO_2's anticancer properties by increasing ROS production, inducing oxidative stress, and promoting apoptosis in cancer cells. While other metals like zinc, copper, or iron have been explored as TiO_2 dopants, strontium and cobalt offer a more balanced combination of enhanced therapeutic efficacy, biocompatibility, and safety, making them ideal choices for TiO_2 doping in advanced biomedical applications, including drug delivery, wound healing, anticancer therapy, and infection control [16–19].

Combining curcumin with dual-metal-doped metal oxide nanoparticles, such as TiO_2 doped with strontium and cobalt, enhances its therapeutic potential. Curcumin's natural anti-inflammatory, antioxidant, anticancer, and antimicrobial properties are amplified by the synergistic effects of the metal dopants, which improve photocatalytic activity, ROS generation, and stability. The dual doping also increases curcumin's bioavailability and reduces its cytotoxicity, making it safer for clinical use. Additionally, these nanoparticles can be functionalized for targeted delivery, improving the effectiveness of treatments for cancer, infections, and wound healing [20–25].

Thus, dual metal ions as Sr/Co ion doping and curcumin coating of TiO_2, TiO_2SrCoCur is synthesized via a simple wet-chemical synthesis process. It is subsequently analyzed using various systematic methods, including XRD, FTIR, DLS, TEM, XPS, UV, and PL, along with its antibacterial, antioxidant, and antifungal activities. In this study, we investigated the anticancer activity in human liver cancer (HepG2) cells, antibacterial activity in G+ and G- bacteria, antifungal activity in *C. albicans* and antioxidant in Trolox free radicals.

2. Materials and methods

2.1. Required Chemical reagents

The chemical reagents such as Titanium isopropoxide ($Ti(OiPr)_4$), Strontium nitrate ($Sr(NO_3)_2$), Cobalt nitrate ($Co(NO_3)_2$), Sodium hydroxide (NaOH), Ethanol (99 %), Curcumin are purchase from Sigma Aldrich, India.

2.2. Synthesis of curcumin coated Sr/Co doped TiO_2 NPs

To synthesize strontium and cobalt doped curcumin-coated TiO_2 nanoparticles, titanium isopropoxide is first dissolved in ethanol (99 %) to form a clear solution, typically at a concentration of 0.090 M. Strontium nitrate and cobalt nitrate are separately dissolved in distilled water to prepare their respective solutions at concentrations of 0.005 M and 0.005 M, respectively. These metal salt solutions are then added dropwise to the titanium precursor solution while stirring to allow the incorporation of Sr and Co ions into the TiO_2 matrix. Sodium hydroxide (NaOH) solution (0.1 M) is slowly added to the mixture to adjust the pH to around 9, causing precipitation of TiO_2. The precipitate is then filtered, washed multiple times with distilled water to remove excess ions and impurities, and dried at 60–80 °C for 6–12 h. The dried material is calcined at 400–500 °C for 2–4 h to transform the titanium hydroxide into crystalline TiO_2, incorporating Sr and Co into the TiO_2 structure. Afterward, curcumin (0.1 M) is dissolved in ethanol to form a solution, and the calcined Sr-Co-doped TiO_2 nanoparticles are dispersed in this curcumin solution. The mixture is subjected to sonication for uniform dispersion, followed by stirring for several hours to allow curcumin to adsorb onto the nanoparticle surface. Finally, the curcumin-coated Sr-Co-doped TiO_2 nanoparticles are dried at 50–60 °C for 6–12 h. The synthesized nanoparticles are characterized using various techniques.

3. Results and discussion

The crystalline size and phase of the synthesized materials were evaluated using the XRD technique. The characteristic peaks in Fig. 1a for synthesized TiO_2SrCoCur at $2\theta = 25.1°$, 37.2°, 48.1°, 54.1°, 54.6°, 55.0, 63.5°, and 68.9° are attributed to TiO_2 with anatase phase (JCPDS #PDF 71–1166), which can be allocated to the crystal lattice planes (101), (004), (200), (211), (116), and (220). The peaks at 27.3°, 42.1°, and 52.8° correspond to the Sr metal hexagonal crystal structure of (110), (220), and (222) planes (JCPDS #PDF 15–0306), respectively. The characteristic peaks at 43.6° and 77.1° correspond to Co metal cubic crystal structures of the (111) and (220) planes, respectively. Furthermore, the peaks at 17.1°, 24.1°, and 32.7° are due to curcumin components. This result is consistent with previous research findings [33–36]. This implies that the synthesized TiO_2SrCoCur NPs consisting anatase phase along with Sr/Co/Cur. Scherrer's equation yields a crystallite size of 33.8 nm.

The FTIR peaks of curcumin at 3425, 2928, 2026, 1628, 1409, 1274, 1153, 1025, 1116, 830, 672, and 619 cm^{-1} correspond to various functional groups and vibrations in the molecule. The peak at 3425 cm^{-1} indicates the O—H stretch of phenolic groups, while the 2928 cm^{-1} peak is due to C—H stretching in methyl and methylene groups. The 1628 cm^{-1} peak represents C═C stretching, typical of aromatic structures, and 1409 cm^{-1} corresponds to C—H bending. Peaks at 1274, 1153, and 1025 cm^{-1} are related to C—O stretching, and 830, 672, and 619 cm^{-1} are attributed to C—H bending vibrations in the aromatic ring. These peaks confirm the presence of hydroxyl, aromatic, and ester functional groups in curcumin, which are essential for its chemical properties [26].

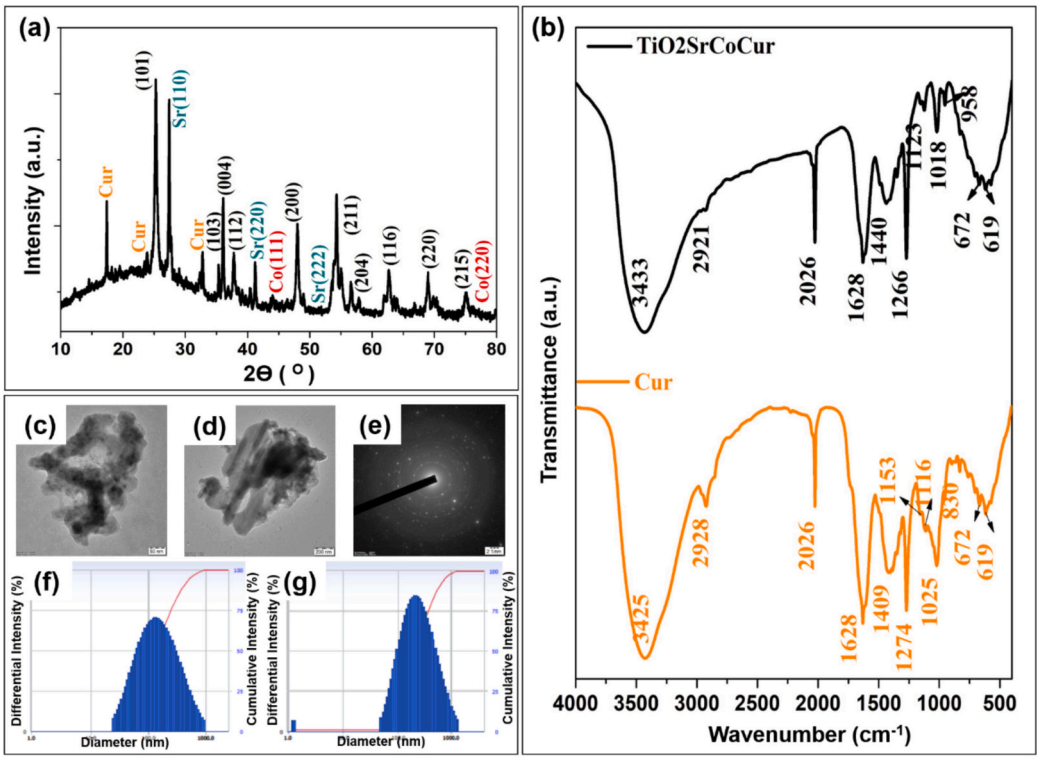

Fig. 1. (a) XRD pattern of TiO_2SrCoCur. (b) FTIR Spectra of TiO_2SrCoCur (black line) and Curcumin (orange line). (c/d) TEM images of TiO_2SrCoCur. (e) SAED pattern of TiO_2SrCoCur. (f/g) DLS spectra of Curcumin and TiO2SrCoCur.

The FTIR peaks for Sr/Co-doped curcumin-coated TiO_2 at 3433, 2921, 2026, 1628, 1440, 1266, 1123, 1018, 958, 672, and 619 cm^{-1} reveal various functional group vibrations and bonding interactions in the material. The peak at 3433 cm^{-1} is linked to the O—H stretch from hydroxyl groups found in both curcumin and the surface hydroxyls on TiO_2. The 2921 cm^{-1} peak corresponds to C—H stretching vibrations from methyl and methylene groups in curcumin. At 2026 cm^{-1}, C═O stretching vibrations are present, indicating ester groups in curcumin. The 1628 cm^{-1} peak reflects aromatic C═C stretches, characteristic of curcumin's backbone, while the 1440 cm^{-1} peak is related to C—H bending from both curcumin and the TiO_2 matrix. The 1266 cm^{-1} peak is attributed to C—O stretching in ester functional groups in curcumin. The 1123 cm^{-1} peak is associated with Ti—O bond vibrations, common in TiO_2 composites. The 1018 cm^{-1} peak corresponds to C—H bending from curcumin's aromatic rings, while the 958 cm^{-1} peak is likely from Ti—O bending or stretching vibrations. Lastly, the peaks at 672 and 619 cm^{-1} suggest bending vibrations in curcumin's aromatic rings or Ti—O interactions. These FTIR findings confirm the successful incorporation of curcumin and the dual metal dopants (Sr and Co) into the TiO_2 structure [18,34,35].

TEM analysis was used to further assess the morphology and nanostructured properties. Small spherically-shaped particles are agglomerated and covered by curcumin layer, as seen in Figs. 1c and d. The TiO_2SrCoCur particles were found to be 36.2 nm (median). SAED pattern shown in Fig. 1e well matches with the XRD pattern. The DLS of Cur and TiO_2SrCoCur, is illustrated in Fig. 1f and g, respectively. The hydrodynamic diameter and polydispersity index of the TiO_2SrCoCur particle were measured and found to be 224 nm and 0.375. The sizeof the particle is higher compared to the results from XRD/TEM analyses may result from the hydrated curcumin matrix absorbing water molecules during DLS spectral analysis [19]. This occurrence can be accredited to the presence of various functional groups, which induce distortion on the Sr/Co-doped TiO_2 surface. These functional groups contribute to electrostatic interactions or enhance the development of intmaolecular H-bonds within the curcumin.

The surface characteristics of the synthesized TiO_2SrCoCur nanoparticles were analyzed utilizing XPS. The core-level spectra for each elements are illustrated in Fig. 2(a–e), confirming the existence of Ti, Sr, Co, C, and O in the TiO_2SrCoCur composition. The deconvoluted spectrum of Ti 2p exhibits a single spin-orbit doublet, as displayed in Fig. 2a. The peak at approximately 458.0 eV, corresponds to Ti 2p3/2, while the second peak, around 463.7 eV, is attributed to Ti 2p1/2 [37,38].

Figs. 2b and 2c reveal that the dopant spectra for Sr 3d and Co 2p can be divided into a primary and a secondary component. The prominent peaks at 132.7 eV and 779.0 eV correspond to the Sr and Co elements integrated within the lattice structure, respectively. 134.8 eV and 780.3 eV peaks are due to trace amounts of Sr and Co oxide derivatives. The narrow-scan XPS spectra for C 1 s and O 1 s are presented in Figs. 2d and 2e, respectively. For C1s, the dominant peak at 284.7 eV is accredited to C sp^2, while the smaller peak at 286.4 eV and 288.6 eV are related with C═O/C—O—C and —COOH [39,40]. It is possible to deconvolute the O 1 s spectra (Fig. 2e) into three components at 530.9, 533.3 and 533.7 eV, which are attributed to lattice oxygen in TiO_2/Sr-Co oxide derivatives and C=O/C-O-C/OH in Cur. Further, the element analysis was done using EDX method. EDX spectrum of TiO_2SrCoCur NPs shown in Fig. 2 g and SEM image and line profile is displayed in Fig. 2 f. The spherical morphology is observed similar to the TEM results. The EDX spectrum shows the presence of Ti, Sr, Co, C and O elements, which is consistent with the XPS results. These results confirmed that the as-synthesized TiO_2SrCoCur NP is composed of the Ti, Sr, Co, C and O components [27–30].

Using PL and UV–Vis spectroscopy techniques, we investigated the optical properties of curcumin and TiO_2SrCoCur. Fig. 3a displays the UV spectra of curcumin and TiO_2SrCoCur. The TiO_2SrCoCur nanocomposite displays absorption peaks at 230 nm and 286 nm, while pristine curcumin shows prominent absorption at 225 nm and a weaker peak at 397 nm, corresponding to its typical absorption region. The incorporation of Sr/Co/Cur into TiO_2 modifies the optical properties associated with electronic transitions. The UV–Vis spectra of TiO_2SrCoCur confirm the existence of Sr/Co/Cur on TiO_2through the absorption peaks at 230 nm

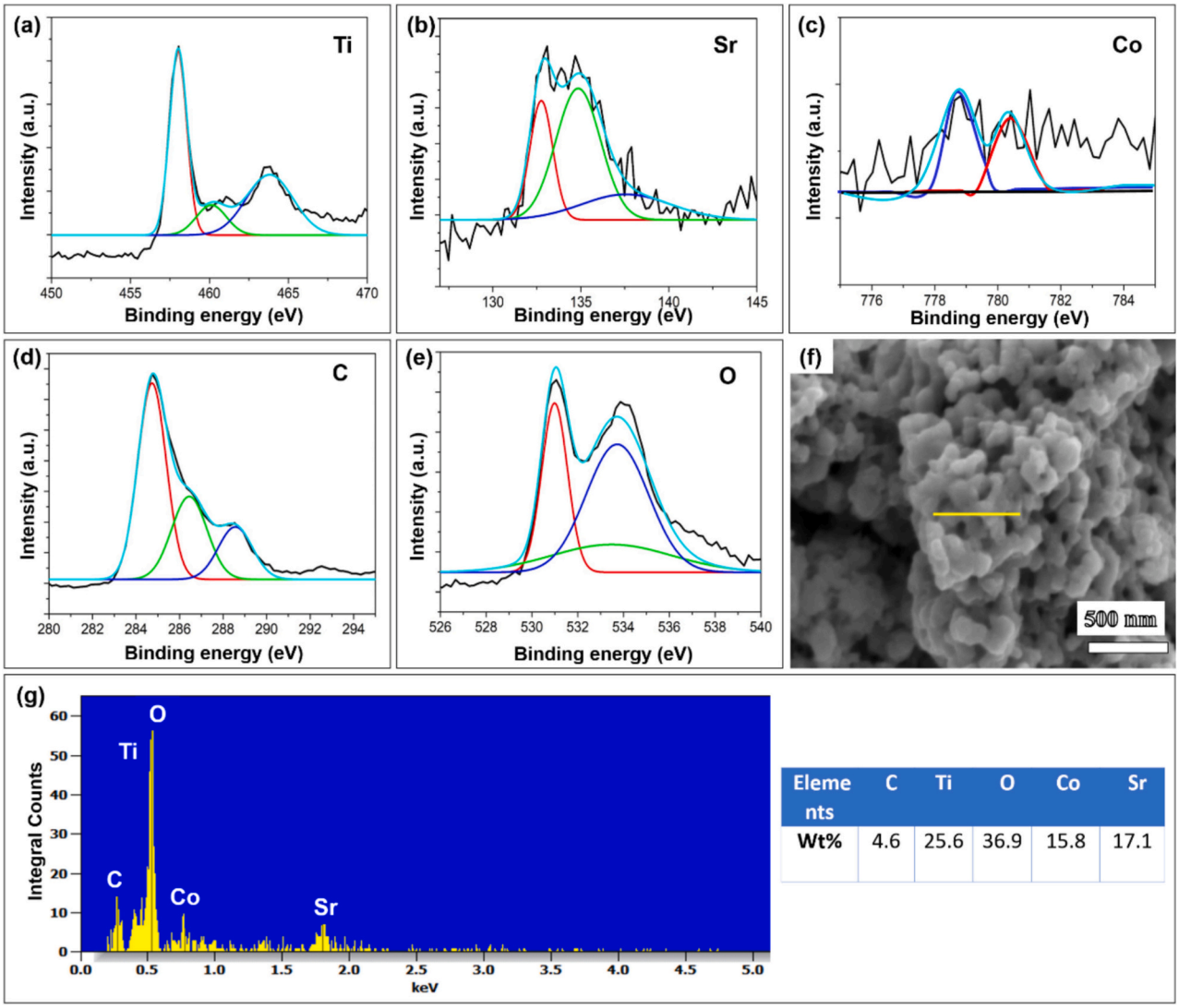

Fig. 2. (a-e) High-Confinement XPS spectrum of TiO_2SrCoCur. (f) SEM of TiO_2SrCoCur NPs (Yellow line represents EDX scanning line profile). (g) EDX line spectra of TiO_2SrCoCur NPs.

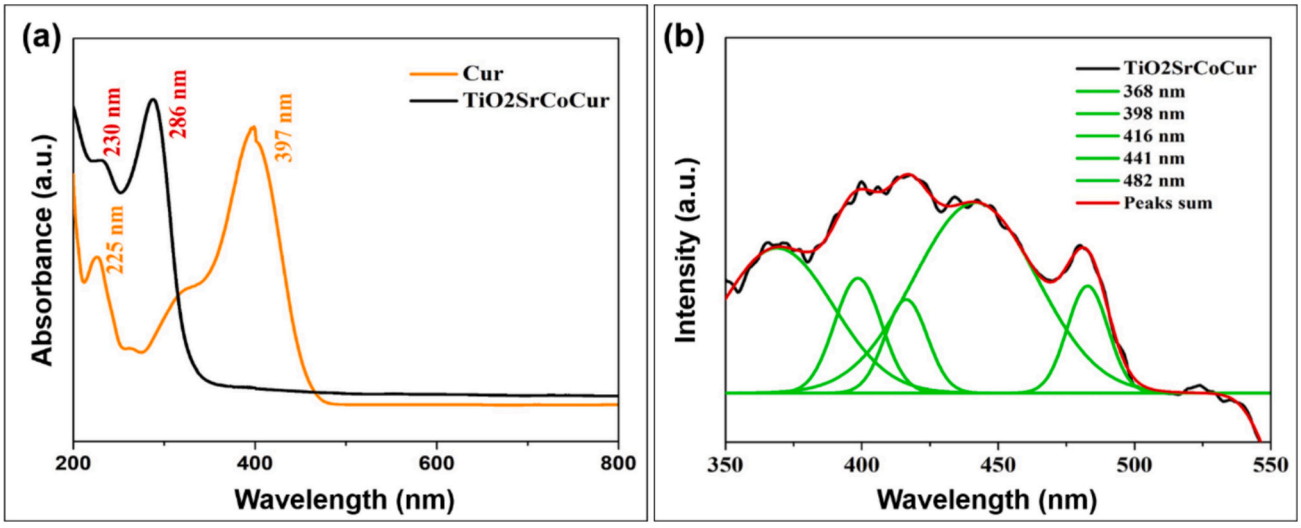

Fig. 3. (a) UV–Vis spectra of TiO_2SrCoCur and curcumin. (b) PL spectrum of TiO_2SrCoCur.

and 286 nm [18,41].

The PL peaks (Fig. 3b) observed at 368, 398, 416, 441, and 482 nm in $TiO_2SrCoCur$ provide valuable insights into its optical properties and electronic transitions. The peak at 368 nm is typically linked to intrinsic electronic transitions in the TiO_2 structure, associated with bandgap excitation. The 398 nm peak likely arises from defect states in the TiO_2 lattice, such as oxygen vacancies or Ti interstitials, which are known to influence photoluminescence. The 416 nm peak could result from a combination of intrinsic transitions and surface defects, possibly related to Sr and Co doping, which introduce new energy levels within the bandgap. The 441 nm peak is likely connected to energy states formed by the doping process, where Sr and Co influence the electronic structure, enhancing the recombination of electron-hole pairs. The 482 nm peak may correspond to deeper energy levels due to the curcumin coating or additional surface defects, contributing to a longer-wavelength emission. These findings suggest that the Sr/Co doping and curcumin coating significantly alter the electronic structure of TiO_2, creating surface defects and modifying its photophysical properties, which could be beneficial for applications in photocatalysis, antibacterial treatments, and anticancer therapies [23,24].

Tested at a concentration of 2 μg/mL against a range of bacterial strains, including *S. aureus, B. subtilis, B. megaterium, K. pneumoniae, P. vulgaris,* and *V. cholera*, were TiO_2, TiO_2SrCo, curcumin, $TiO_2SrCoCur$, and amoxcillin (Fig. 4a). The inhibition zone by the well diffusion approach is displayed in Fig. 4a. The inhibition zone of $TiO_2SrCoCur$ is greater than 12.3 mm for each strain of bacteria. It's remarkable to note

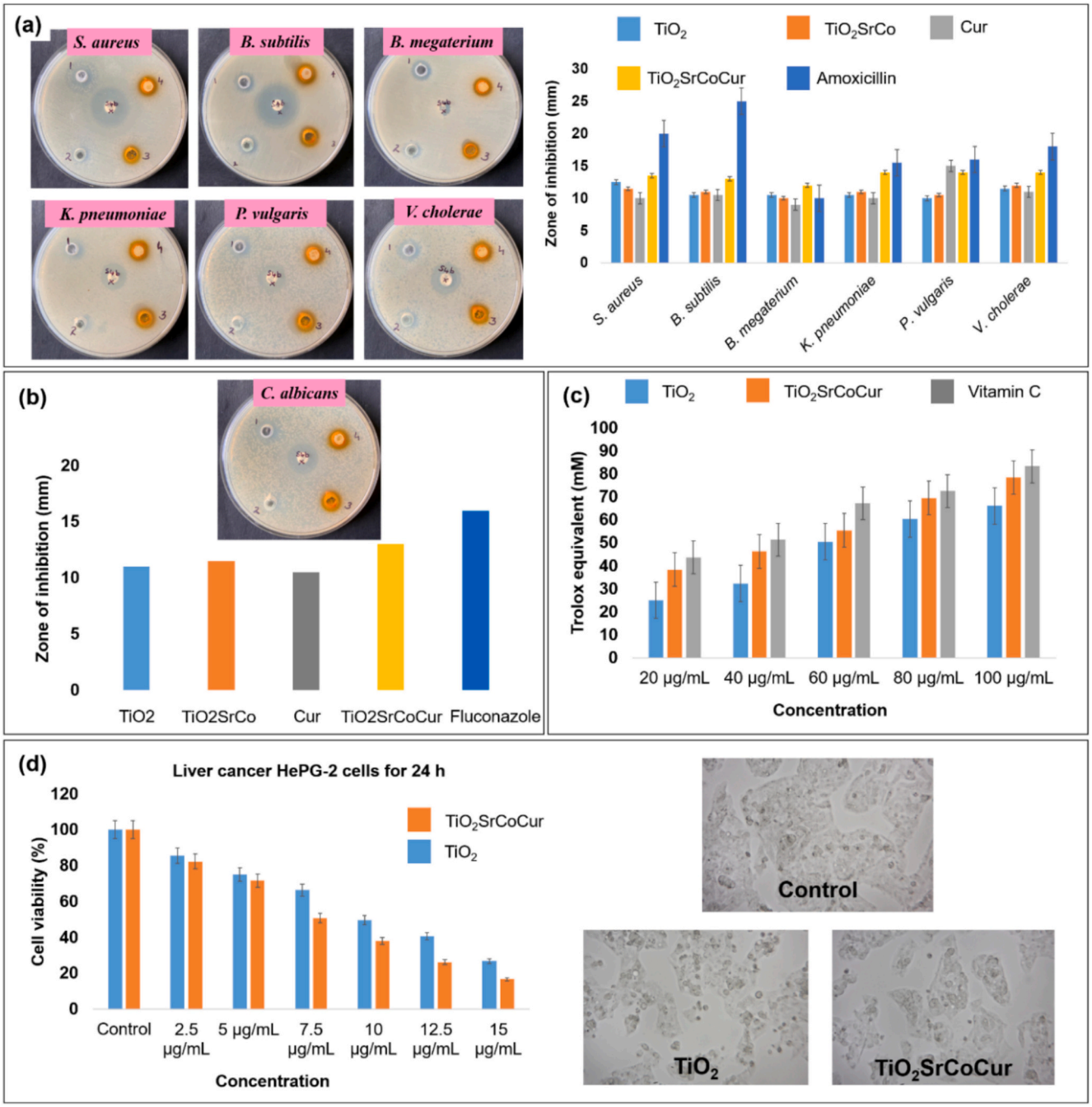

Fig. 4. (a) Activity of TiO_2, TiO_2SrCo, Cur, $TiO_2SrCoCur$ and Amoxcillin against bacterial strains (b) Activity of TiO_2, TiO_2SrCo, Curcumin, $TiO_2SrCoCur$ and Fluconazole against *C. albicans* (c) Antioxidant activity of TiO_2, $TiO_2SrCoCur$ and vitamin-C. (d) Anticancer activity of $TiO_2$and $TiO_2SrCoCur$ NPs on HePG-2 cells.

that the zone of inhibition for *K. pneumoniae, P. vulgaris,* and *V. cholera* is demonstrated to be greater (14.2 mm) than that of its counterparts. The antibacterial effectiveness against *K. pneumoniae* was nearly equal to that of the widely used medicine amoxicillin. The observed increased zone of inhibition (12.3–14.2 mm) could point to potential antibacterial properties of the as-synthesized TiO_2SrCoCur NPs. The antibacterial effectiveness of TiO_2SrCoCur nanoparticles largely relies on the synergistic interaction among Sr, Co, and curcumin components when compared to pristine TiO_2, curcumin, and TiO_2SrCo. The presence of Sr^{2+}, Ti^{2+}, and Co^{2+} ions, along with factors such as ratio of surface/volume, charge interactions, and enhanced transmission capacity for reactive molecules, enables these components to generate oxidative stress within bacterial cells [31,32,42].

As noted earlier, surface defects, particularly oxygen vacancies on TiO_2SrCoCur, significantly influence the biocidal properties, as shown in the PL analysis. These defects increase the generation of hydroxide radicals and ROS through a water-splitting mechanism, which subsequently enhances the antibacterial activity. TiO_2SrCoCur NPs are effective in disrupting biofilm formation, damaging bacterial cell, and releasing ROS, initiating to the inhibition of bacterial growth. So, TiO_2SrCoCur nanoparticles hold promise for combating various microorganisms in biomedical field. Additionally, TiO_2SrCoCur NPs might assistance in wound healing and infection prevention. However, factors such as particle composition, size, concentration, and bacterial strain type can influence the antibacterial efficacy. Further studies are required to comprehensively evaluate their potential and broaden their applications.

Using the in vitro experimental model, we further examined TiO_2SrCoCur's antifungal activity. The antifungal activity of TiO_2, TiO_2SrCo, fluconazole, curcumin, and TiO_2SrCoCur against *Candida albicans* is displayed in Fig. 4b. The results indicate that TiO_2SrCoCur exhibits a maximum inhibition zone of 16.1 mm, outperforming its synthetic counterparts. TiO_2SrCoCur nanoparticles also demonstrated a dose-dependent ability to scavenge free radicals. The study highlighted the effectiveness of TiO_2SrCoCur NPs in comparison to Trolox for free radical scavenging, showcasing their role in controlling oxidative stress, preventing membrane degradation, and maintaining cellular integrity. Fig. 4c illustrates the antioxidant properties of the synthesized TiO_2 and TiO_2SrCoCur materials alongside the commonly used antioxidant, vitamin C. The Trolox free radical scavenging activity ranged from 37 % to 78 % at concentrations between 20 and 100 μg/mL. When it came to the ability of vitamin C, at 100 μg/mL, to scavenge free radicals produced by Trolox, it was nearly identical. The efficiency of TiO_2's fungicidal action is dependent on a number of factors, including the methods used to create the nanoparticles, their concentration, duration of treatment, and chemical stability. Given that TiO_2 is synthesized using the biomolecule curcumin matrix, their size and bioactive components might be able to reveal whether or not they significantly inhibit fungal infections in tests [43–48]. The creation of ROS is one of the factors taken into consideration for TiO_2SrCoCur's antioxidant capabilities.

As shown in Fig. 4d, experiments were conducted using varying concentrations of TiO_2SrCoCur NPs on HePG-2 cell lines, a cell line used to study liver cancer activities (for 24 h). The photomicrograph (20×) in Fig. 4d-insets shows the cellular changes as compared to TiO_2 and control when HePG-2 cells are treated with TiO_2SrCoCur (2.5, 5, 7.5, 10, 12.5, and 15 μg/mL). The control cell remains in its normal shape and has 100 % cell viability without treatment. On liver cancer cells, TiO_2SrCoCur NPs had a significant anti-proliferative effect. TiO_2SrCoCur was shown to exhibit a more favourable cytotoxic response than pure TiO_2. The reduction in cell viability observed with TiO_2SrCoCur NPs may be ascribed to the interaction between curcumin and TiO_2 molecules, having a matrix form. The lower cell viability observed in TiO_2SrCoCur compared to pure TiO_2 can be attributed to several factors. Firstly, the dual doping of strontium (Sr) and cobalt (Co) in TiO_2 enhances its photocatalytic activity, which is known to generate ROS upon exposure to light. These ROS can induce oxidative stress within cancer cells, leading to DNA damage, apoptosis, or necrosis, thereby reducing cell viability. The curcumin coating on TiO_2 further amplifies this effect, as curcumin itself has proven anticancer properties, promoting cell cycle arrest and apoptosis in cancer cells. Additionally, the Sr and Co dopants may introduce defects in the TiO_2 lattice, such as oxygen vacancies, which can contribute to increased ROS production and higher anticancer efficacy. The combined effects of these factors enhanced ROS generation due to doping and the therapeutic properties of curcumin make TiO_2SrCoCur a more effective anticancer agent compared to pure TiO_2, leading to reduced cancer cell viability.

4. Conclusion

The TiO_2SrCoCur NPs synthesized in this study presents a promising multifunctional material with enhanced antibacterial properties, attributable to the synergistic effects of Sr and Co co-doping and surface functionalization with curcumin. The prominent green emission observed in the PL spectrum indicates a high density of oxygen vacancies, which are known to promote ROS generation, thereby boosting antimicrobial activity. Compared to undoped or singly doped TiO_2 systems reported in previous studies, the co-doped curcumin-coated composite exhibited superior performance, highlighting the advantage of multicomponent modification. Furthermore, the long-term colloidal stability observed through DLS analysis suggests practical applicability in aqueous environments. The NPs and their variants demonstrated potent antibacterial activity against both Gram-positive and Gram-negative bacterial strains, with efficacy increasing at higher concentrations (increased zone of inhibition 12.3–14.2 mm). Additionally, TiO_2SrCoCur was evaluated for its antioxidant properties using Trolox free radicals and for antifungal activity against *C. albicans* (maximum inhibition zone of 16.1 mm). Notably, TiO_2SrCoCur exhibited promising anticancer effects against liver cancer (HePG-2) cells, requiring a lower inhibitory concentration for efficacy ($IC_{50} \approx 7.5$ μg/mL).

Overall, the synthesized TiO_2SrCoCur NPs hold significant potential for biomedical applications, including future developments in anticancer, antioxidant, antibacterial, and antifungal therapies. Further research should explore their use in targeted drug delivery, wound healing, and medical coatings, as well as assess their in vivo efficacy in cancer and infection treatments. Improving their bioavailability and clinical safety will be essential for advancing these NPs into therapeutic applications.

CRediT authorship contribution statement

Shivangi Gupta: Conceptualization. **R. Roopashree:** Formal analysis. **Vivek Saraswat:** Methodology. **Shivangi Giri:** Software. **Jagmeet Sohal:** Writing – original draft. **Thalakulam Shanmugam Boopathi:** Resources. **Fatimah S. Al-Khattaf:** Data curation. **Ashraf Atef Hatamleh:** Visualization. **Tingting Qiao:** Investigation.

Declaration of competing interest

The authors declare that they have no known competing financial interests or personal relationships that could have appeared to influence the work reported in this paper.

Appendix A. Supplementary data

Supplementary data to this article can be found online at https://doi.org/10.1016/j.inoche.2025.115060.

Data availability

No data was used for the research described in the article.

References

[1] T. Indumathi, N. Krishnamoorthy, R. Valarmathy, K. Saraswathi, S. Dilwyn, S. Prabhu, Green synthesis of α-Fe 2 O 3 nanoparticles mediated Musa Acuminata: a study of their applications as photocatalytic degradation and antibacterial agent, Nano Biomed. Eng. 14 (3) (2022).

[2] Xiuli Liang, Xiaojun Zhang, Kaiqi Lian, Xiuhua Tian, Mingliang Zhang, Shiqiong Wang, Cheng Chen, et al., Antiviral effects of bovine antimicrobial peptide against TGEV in vivo and in vitro, J. Vet. Sci. 21 (5) (2020) e80.

[3] Hong-jie Li, Dong-sheng Gao, Yong-tao Li, Yong-sheng Wang, Hong-ying Liu, Jun Zhao, Antiviral effect of lithium chloride on porcine epidemic diarrhea virus in vitro, Res. Vet. Sci. 118 (2018) 288–294.

[4] Yichen Jian, Shijie Li, Dongliang Li, Changshen Ning, Sumei Zhang, Fuchun Jian, Hongbin Si, Evaluation of the in vitro acaricidal activity of ethanol extracts of seven Chinese medicinal herbs on Ornithonyssus sylviarum (Acari: Macronyssidae), Exp. Appl. Acarol. 87 (1) (2022) 67–79.

[5] Xin Wang, Wu Yong, Ze-yu Wang, Jin-jie Li, Wen Li, Qian Li, Na Luan, Xiao-ya Shang, Anti-inflammatory iridoid glycosides from fruits of Cornus officinalis, Phytochem. Lett. 52 (2022) 122–125.

[6] Chao Tong, Tong Chen, Zewen Chen, Hao Wang, Xuefang Wang, Fang Liu, Hongyu Dai, Xuebing Wang, Xiao Li, Forsythiaside a plays an anti-inflammatory role in LPS-induced mastitis in a mouse model by modulating the MAPK and NF-κB signaling pathways, Res. Vet. Sci. 136 (2021) 390–395.

[7] M.R. Amiri, M. Alavi, M. Taran, D. Kahrizi, Antibacterial, antifungal, antiviral, and photocatalytic activities of TiO2 nanoparticles, nanocomposites, and bio-nanocomposites: recent advances and challenges, J. Public Health Res. 11 (2) (2022), https://doi.org/10.1177/22799036221104151.

[8] S. Pandeya, R. Ding, Y. Ma, Z. Li, M.K. Joshi, Self-standing CdS/TiO2 Janus nanofiberous membrane: COD removal, antibacterial activity and photocatalytic degradation of organic pollutants, J. Environ. Chem. Eng. (2024).

[9] N. Cioffi, M. Rai, Nano-antimicrobials, in: M. Rai Nicola Cioffi (Ed.), Synthesis and Characterization of Novel Nano Antimicrobials, Springer, Berlin Heidelberg, 2012.

[10] A. Zaleska, Doped-TiO2: a review, Recent Pat. Eng. 2 (2008) 157–164.

[11] M.N. Alomary, M.A. Ansari, Proanthocyanin-capped biogenic TiO2 nanoparticles with enhanced penetration, antibacterial and ROS mediated inhibition of bacteria proliferation and biofilm formation: a comparative approach, Chem. Eur. J. 27 (18) (2021) 5817–5829.

[12] K. Indira, et al., Synthesis of titanium/niobium oxide nanocomposite on top open bamboo like titanium dioxide nanotube for the catalytic degradation of organic pollutants, J. Environ. Chem. Eng. 9 (2021) 105400.

[13] S. Ahmadpour Kermani, S. Salari, P. Ghasemi Nejad Almani, Comparison of antifungal and cytotoxicity activities of titanium dioxide and zinc oxide nanoparticles with amphotericin B against different Candida species: in vitro evaluation, J. Clin. Lab. Anal. 35 (1) (2021) e23577.

[14] R. Hernandez, A. Jimenez-Chávez, A. De Vizcaya, J.A. Lozano-Alvarez, K. Esquivel, I.E. Medina-Ramírez, Synthesis of TiO2-Cu2+/CuI nanocomposites and evaluation of antifungal and cytotoxic activity, Nanomaterials 2023 (1900) 13, https://doi.org/10.3390/nano13131900.

[15] Y. Xing, R. Yi, H. Yang, Q. Xu, R. Huang, J. Tang, X. Li, X. Liu, L. Wu, X. Liao, X. Bi, J. Yu, Antifungal effect of chitosan/Nano-TiO2 composite coatings against Colletotrichum gloeosporioides, Cladosporium oxysporum and Penicillium steckii, Molecules 26 (15) (2021) 4401, https://doi.org/10.3390/molecules26154401.

[16] Suchita C. Warangkar, Manish R. Deshpande, Narayan D. Totewad, Archana A. Singh, Antibacterial, Antifungal and Antiviral Nanocomposites: Recent Advances and Mechanisms of Action, 2022, https://doi.org/10.5772/intechopen.108994.

[17] P.C.L. Muraro, R.D. Wouters, G.P. Chuy, et al., Titanium dioxide nanoparticles: green synthesis, characterization, and antimicrobial/photocatalytic activity, Biomass Convers. Biorefinery (2023), https://doi.org/10.1007/s13399-023-04542-w.

[18] A.N. El-Shazly, G.S. El-Sayyad, A.H. Hegazy, et al., Superior visible light antimicrobial performance of facet engineered cobalt doped TiO2 mesocrystals in pathogenic bacterium and fungi, Sci. Rep. 11 (2021) 5609, https://doi.org/10.1038/s41598-021-84989-x.

[19] M. Shabib Akhtar, K. Chandrasekaran, S. Saminathan, et al., Nanoengineered chitosan functionalized titanium dioxide biohybrids for bacterial infections and cancer therapy, Sci. Rep. 14 (2024) 3705, https://doi.org/10.1038/s41598-024-52847-1.

[20] J.H. Zhou, L. Zhao, Multifunction Sr, Co and F co-doped microporous coating on titanium of antibacterial, angiogenic and osteogenic activities, Sci. Rep. 6 (2016) 29069.

[21] J. Zhou, X. Wang, L. Zhao, Antibacterial, angiogenic, and osteogenic activities of Ca, P, Co, F, and Sr compound doped titania coatings with different Sr content, Sci. Rep. 9 (2019) 14203, https://doi.org/10.1038/s41598-019-50496-3.

[22] Mauro F. La Russa, Andrea Macchia, Silvestro A. Ruffolo, Filomena De Leo, Marianna Barberio, Pasquale Barone, Gino M. Crisci, Clara Urzì, Testing the antibacterial activity of doped TiO2 for preventing biodeterioration of cultural heritage building materials, Int. Biodeterior. Biodegradation 96 (2014) 87–96.

[23] Xuejiao Zhang, Yong Huang, Bingbing Wang, Xiaotong Chang, Hao Yang, Jinping Lan, Saisai Wang, Haixia Qiao, He Lin, Shuguang Han, Yaxiong Guo, Xiaojun Zhang, A functionalized Sm/Sr doped TiO2 nanotube array on titanium implant enables exceptional bone-implant integration and also self-antibacterial activity, Ceram. Int. 46 (10, Part A) (2020) 14796–14807.

[24] Changjiang Pan, Tingting Liu, Ya Yang, Tao Liu, Zhihao Gong, Yanchun Wei, Li Quan, Zhongmei Yang, Sen Liu, Corporation of Sr2+ and Ag nanoparticles into TiO2 nanotubes to synergistically enhance osteogenic and antibacterial activities for bone repair, Mater. Des. 196 (2020) 109086.

[25] M. Ali, R. Hussain, F. Tariq, et al., Highly effective visible light-activated cobalt-doped TiO2 nanoparticles for antibacterial coatings against campylobacter jejuni, Appl. Nanosci. 10 (2020) 1005–1012, https://doi.org/10.1007/s13204-019-01193-0.

[26] W. Zhang, et al., Effects of strontium in modified biomaterials, Acta Biomater. 7 (2011) 800–808.

[27] D. Guo, K. Xu, Y. Han, The influence of Sr doses on the in vitro biocompatibility and in vivo degradability of single-phase Sr-incorporated HAP cement, J. Biomed. Mater. Res. A 86A (2008) 947–958.

[28] S. Saha, K. Pramanik, A. Biswas, Antibacterial activity and biocompatibility of curcumin/TiO2 nanotube array system on Ti6Al4V bone implants, Mater. Technol. 36 (4) (2021) 221–232, https://doi.org/10.1080/10667857.2020.1742984.

[29] D. Zheng, C. Huang, H. Huang, Y. Zhao, M.R.U. Khan, H. Zhao, L. Huang, Antibacterial mechanism of curcumin: a review, C&B 17 (2020) e2000171, https://doi.org/10.1002/cbdv.202000171.

[30] Q. Guo, P. Li, Y. Zhang, et al., Polydopamine-curcumin coating of titanium for remarkable antibacterial activity via synergistic photodynamic and photothermal properties, Photochem. Photobiol. 00 (2023) 1–13, https://doi.org/10.1111/php.13870.

[31] Chandrasekaran Karthikeyan, Tippabattini Jayaramudu, Dariela Núñez, Nery Jara, Andres Opazo-Capurro, Kokkarachedu Varaprasad, Kyobum Kim, Murali M. Yallapu, Rotimi Sadiku, Hybrid nanomaterial composed of chitosan, curcumin, ZnO and TiO2 for antibacterial therapies, Int. J. Biol. Macromol. 242 (Part 2) (2023) 124814.

[32] K. Varaprasad, M. López, D. Núñez, T. Jayaramudu, E.R. Sadiku, C. Karthikeyan, P. Oyarzúnc, Antibiotic copper oxide-curcumin nanomaterials for antibacterial applications, J. Mol. Liq. 300 (2020) 112353, https://doi.org/10.1016/J.MOLLIQ.2019.112353.

[33] D. Reyes-Coronado, G. Rodríguez-Gattorno, M.E. Espinosa-Pesqueira, C. Cab, R. Coss, G. Oskam, Phase-pure TiO(2) nanoparticles: anatase, brookite and rutile, Nanotechnology 19 (2008) 145605.

[34] S.W.L. Silva, M.A. Lansarin, C.C. Moro, Synthesis, characterization and photocatalytic activity of nanostructured TiO2 catalysts doped with metals, Quím. Nova 36 (2013) 382–386.

[35] S.K.S. Angshuman Ray Chowdhuri, D. Laha, S. Pal, P. Karmakar, One-pot synthesis of folic acid encapsulated upconversion nanoscale metal organic frameworks for targeting, imaging and pH responsive drug release, Dalton Trans. 45 (2016) 18120–18132.

[36] C. Karthikeyan, et al., Size-dependent cellular uptake of sodium alginate passivated tin dioxide nanoparticles in triple-negative breast cancer cells, J. Ind. Eng. Chem. 123 (2023) 476–487.

[37] J. Suriyaprakash, Y.B. Xu, Y.L. Zhu, et al., Designing of metallic nanocrystals embedded in non-stoichiometric perovskite nanomaterial and its surface-electronic characteristics, Sci. Rep. 7 (2017) 8343, https://doi.org/10.1038/s41598-017-09031-5.

[38] Chunyan Wang, Lianwei Shan, Dongyuan Song, Yanwei Xiao, Jagadeesh Suriyaprakash, Hydrothermal synthesis of rGO/PbTiO3 photocatalyst and its photocatalytic H2 evolution activity, J. Nanomater. 4869728 (2019) 9.

[39] Jagadeesh Suriyaprakash, Kanchan Bala, Lianwei Shan, Wu Lijun, Neeraj Gupta, Molecular engineered carbon-based sensor for ultrafast and specific detection of neurotransmitters, ACS Appl. Mater. Interfaces 13 (51) (2021) 60878–60893.

[40] Jagadeesh Suriyaprakash, Lianwei Shan, Neeraj Gupta, Hao Wang, Lijun Wu, Janus 2D-carbon nanocomposite-based ascorbic acid sensing device: experimental and theoretical approaches, Compos. Part B Eng. 245 (2022) 110233.

[41] Thangavelu Indumathi, Jagadeesh Suriyaprakash, Abdullah A. Alarfaj, Abdurahman Hajinur Hirad, Ravindran Jaganathan, Maghimaa Mathanmohun, Synergistic effects of CuO/TiO2-chitosan-farnesol nanocomposites: synthesis, characterization, antimicrobial, and anticancer activities on melanoma cells SK-MEL-3, J. Basic Microbiol. (2023) 1–14.

[42] Kavina Ganapathy, Vaibhav Rastogi, Chandra Prakash Lora, Jagadeesh Suriyaprakash, Abdullah A. Alarfaj, Abdurahman Hajinur Hirad, T. Indumathi, Biogenic synthesis of dopamine/carboxymethyl cellulose/TiO2 nanoparticles using Psidium guajava leaf extract with enhanced antimicrobial and anticancer activities, Bioprocess Biosyst. Eng. (2023), https://doi.org/10.1007/s00449-023-02954-6.

[43] Wongchai Anupong, Ruangwong On-uma, Kumchai Jutamas, Saleh H. Salmen, Sulaiman Ali Alharbi, G.K. Deepika Joshi, Jhanani., Antibacterial, antifungal, antidiabetic, and antioxidant activities potential of Coleus aromaticus synthesized titanium dioxide nanoparticles, Environ. Res. 216 (Part 3) (2023) 114714.

[44] H. Hu, X. Fan, Y. Yin, Q. Guo, D. Yang, X. Wei, et al., Mechanisms of titanium dioxide nanoparticle-induced oxidative stress and modulation of plasma glucose in mice, Environ. Toxicol. 34 (2019) 1221–1235.

[45] C.-Y. Cheng, A. Haque, M.-F. Hsieh, S. Imran Hassan, M.S.H. Faizi, N. Dege, M. S. Khan, 1,4-Disubstituted 1H-1,2,3-Triazoles for renal diseases: studies of viability, anti-inflammatory, and antioxidant activities, Int. J. Mol. Sci. 21 (2020) 3823, https://doi.org/10.3390/ijms21113823.

[46] Muhammad Asam Raza, et al., Computational modeling of imines based anti-oxidant and anti-esterases compounds: Synthesis, single crystal and In-vitro

assessment, Comput. Biol. Chem. 104 (2023) 107880, https://doi.org/10.1016/j.compbiolchem.2023.107880.
[47] Natarajan Arumugam, et al., Stereoselective synthesis and discovery of novel spirooxindolopyrrolidine engrafted indandione heterocyclic hybrids as antimycobacterial agents, Bioorg. Chem. 110 (2021) 104798, https://doi.org/10.1016/j.bioorg.2021.104798.
[48] Natarajan Arumugam, et al., Regio- and diastereoselective synthesis of spiropyrroloquinoxaline grafted indole heterocyclic hybrids and evaluation of their anti-mycobacterium tuberculosis activity, RSC Adv. 10 (2020) 23522–23531, https://doi.org/10.1039/D0RA02525A.

Shivangi Gupta is a Ph.D. research scholar specializing in interdisciplinary studies that integrate computational chemistry, mathematics, and information technology. With a strong academic background in computer science and advanced research in mathematical modeling and scientific computing, her work focuses on applying algorithmic and AI-driven approaches to chemical data analysis and molecular simulations. She has contributed to research on predictive modeling of chemical processes and material behavior using high-performance computing tools. She has presented her findings at academic forums and is actively involved in collaborative projects that bridge computational science with applied chemistry. Her vision is to foster innovation at the intersection of technology and chemistry to address complex scientific challenges.